

# A non-catalytic role of DNA polymerase $\eta$ in recruiting Rad18 and promoting PCNA monoubiquitination at stalled replication forks

Michael Durando<sup>1,\*</sup>, Satoshi Tateishi<sup>2</sup> and Cyrus Vaziri<sup>1,\*</sup>

<sup>1</sup>Department of Pathology and Laboratory Medicine, University of North Carolina at Chapel Hill, Chapel Hill, NC 27599, USA and <sup>2</sup>Division of Cell Maintenance, Institute of Molecular Embryology and Genetics (IMEG), Kumamoto University, Honjo 2-2-1, Kumamoto 860-0811, Japan

Received August 28, 2012; Revised December 13, 2012; Accepted December 24, 2012

## ABSTRACT

**Trans-lesion DNA synthesis (TLS) is a DNA damage-tolerance mechanism that uses low-fidelity DNA polymerases to replicate damaged DNA. The inherited cancer-predisposition syndrome xeroderma pigmentosum variant (XPV) results from error-prone TLS of UV-damaged DNA. TLS is initiated when the Rad6/Rad18 complex monoubiquitinates proliferating cell nuclear antigen (PCNA), but the basis for recruitment of Rad18 to PCNA is not completely understood. Here, we show that Rad18 is targeted to PCNA by DNA polymerase eta (Pol $\eta$ ), the XPV gene product that is mutated in XPV patients. The C-terminal domain of Pol $\eta$  binds to both Rad18 and PCNA and promotes PCNA monoubiquitination, a function unique to Pol $\eta$  among Y-family TLS polymerases and dissociable from its catalytic activity. Importantly, XPV cells expressing full-length catalytically-inactive Pol $\eta$  exhibit increased recruitment of other error-prone TLS polymerases (Pol $\kappa$  and Pol $\iota$ ) after UV irradiation. These results define a novel non-catalytic role for Pol $\eta$  in promoting PCNA monoubiquitination and provide a new potential mechanism for mutagenesis and genome instability in XPV individuals.**

## INTRODUCTION

Living organisms are constantly exposed to ubiquitous genotoxins from endogenous and external sources (1). However, cells have evolved numerous DNA damage response (DDR) pathways that protect genomic DNA and prevent genetic instability (2). Trans-lesion synthesis (TLS) is a DDR mechanism involving specialized DNA polymerases that can replicate damaged DNA templates (3).

TLS relies on inherently error-prone DNA polymerases of the Y family to replicate damaged DNA (4). TLS by Y-family polymerases (Pol $\eta$ , Pol $\iota$ , Pol $\kappa$  and Rev1) (5) maintains replication in cells harbouring damaged DNA, albeit at the cost of reduced fidelity. Each TLS polymerase performs relatively error-free replication past a preferred cognate lesion; in the absence of the appropriate TLS polymerase for its preferred lesion, mutagenic replication by error-prone polymerases predisposes to genetic instability (2).

Pol $\eta$  is unique among Y-family polymerases in its ability to perform accurate replication past UV-damaged DNA (6,7). Lack of Pol $\eta$  in the inherited cancer-predisposition syndrome xeroderma pigmentosum variant (XPV) (8) results in error-prone replication by other Y-family polymerases in sunlight-exposed cells (9,10). Thus, UV-induced mutagenesis due to Pol $\eta$  deficiency compromises genetic integrity to manifest as exquisite sunlight sensitivity and early skin cancer propensity.

A prerequisite for error-prone replication in TLS is the Rad6/Rad18-mediated monoubiquitination of proliferating cell nuclear antigen (PCNA) at the highly conserved lysine K164 (11,12). Y-family polymerases contain ubiquitin-binding (UBZ) domains that confer affinity to monoubiquitinated PCNA (13,14). Failure to monoubiquitinate PCNA at K164 phenocopies XPV by compromising TLS and sensitizing cells to UV light and other ubiquitous genotoxins (15–18). Several other DDR pathways also depend on PCNA monoubiquitination, including SHPRH/HTLF-mediated template switching (19), ZRANB3-dependent replication fork restart (20), SNM1A-dependent intrastrand cross-link repair (21) and the Fanconi Anaemia pathway activation (22).

Despite its pivotal role in the DDR, the molecular mechanisms regulating Rad18-mediated PCNA monoubiquitination are incompletely understood. The Rad18–Rad6 complex is thought to be recruited to the vicinity of damaged DNA via direct interactions with RPA-coated

\*To whom correspondence should be addressed. Tel: +1 617 818 3441; Fax: +1 919 966 5046; Email: mdurando@med.unc.edu  
Correspondence may also be addressed to Cyrus Vaziri. Tel: +1 919 843 9630; Fax: +1 919 966 5046; Email: cyrus\_vaziri@med.unc.edu  
Present address:

Michael Durando, Department of Pathology and Laboratory Medicine, University of North Carolina at Chapel Hill, Chapel Hill, NC 27599, USA.

ssDNA (23,24). However, Rad18 lacks PCNA-binding motifs, and it is unclear how Rad18 is targeted specifically to PCNA at stalled forks (or other sites of post-replication repair). A recent report by Zou and colleagues (25) identified Spartan as a binding partner of both Rad18 and PCNA and proposed that Spartan acts as a scaffold for recruiting Rad18 to PCNA. Consistent with a role for Spartan in targeting Rad18 to PCNA, those workers found DNA damage-induced PCNA monoubiquitination was modestly attenuated in Spartan-depleted cells. However, several other more recent publications have reported alternative roles for Spartan in DNA damage signalling (26–29), and it is unclear whether Spartan or alternative putative mediators exist to facilitate recruitment of Rad18 to PCNA.

In mammalian cells, Rad18 exists in complex with Pol $\eta$  (30,31), and association of Rad18 with Pol $\eta$  is necessary for normal DNA damage tolerance (30–32). Assembly of the Rad18–Pol $\eta$  complex is stringently controlled by Cdc7 and Chk1 kinases, which serve to integrate TLS with S-phase progression and the S-phase checkpoint, respectively (30,32). Here we report that the Pol $\eta$ –Rad18 interaction plays a key role in targeting Rad18 to PCNA and facilitating efficient PCNA monoubiquitination. Interestingly, the novel role of Pol $\eta$  in stimulation of PCNA monoubiquitination is fully dissociable from its activity as a DNA polymerase. We show that the Pol $\eta$ –Rad18 interaction provides the basis for coupling PCNA monoubiquitination with DNA damage-inducible checkpoint pathways mediated by p53 and Chk1. Our results also provide a potential explanation for numerous reports that Pol $\eta$  confers tolerance of non-cognate lesions (33,34) and that catalytically inactive Pol $\eta$  can partially rescue the DNA damage-sensitivity phenotypes of XPV cells (35,36). Moreover, because some XPV cells express a catalytically inactive Pol $\eta$  that retains the ability to promote PCNA monoubiquitination, our results also indicate a new molecular mechanism for the mutagenesis and cancer propensity of XPV patients.

## MATERIALS AND METHODS

### Cell culture and transfection

H1299, HDF, XP115LO [GM02359(37,38)] and HCT-116 WT and Rad18<sup>-/-</sup> cells (39) were cultured in Dulbecco's modified Eagle medium (DMEM) supplemented with 10% fetal bovine serum (FBS) and penicillin–streptomycin. siRNA and pcDNA, pACCMV and pCAGGS plasmid transfections were done using Lipofectamine 2000 (Invitrogen) as previously described (30).

### Materials, siRNA, plasmid and adenovirus construction

siRNA oligonucleotide sequences were as follows: non-targeting Control, 5'–UAGCGACUAAACACAUC AAUU–3'; Pol $\eta$ , 5'–GCAGAAAGGCAGAAAGUUA–3'; Pol $\eta$ -3' UTR, 5'–CCAUUUAGGUGCUGAGUUA–3'; Pol $\eta$ -5' UTR, 5'–GAAUAAAUCUCGCUCGAAA–3'; Chk1, 5'–GCGUGCCGUAGACUGUCCA–3'; USP1, 5'–TCGGCAATACTTGCTATCTTA–3'; Polk, 5'–GUAAGAGGUUAAGGAAA–3'; Rad18 3' UTR,

5'–UUAUAAAUGCCCAAGGAAAUU–3'; Spartan 5'–ACCGGACUUGCAGGCACUGUUUGUU–3'. CFP was cloned onto the C-terminus of Rad18 in pACCMV using BamHI and XbaI restriction sites. Rad18 and CFP were separated by a linker of the sequence 5'–ACCTCTT CCGGTTCCAGTCCCTGTTCCGGGTCCTGCTCCT ATGCGTATGGCTCC–5'. Rad18- $\Delta$ (402–445) and Rad18-C28F were generated as described previously (31) and cloned into pACCMV using EcoRI and BamHI restriction sites. Pol $\eta$ - $\Delta$ PCNA-interacting peptide (PIP) was cloned into pACCMV using EcoRI and BamHI restriction sites and a C-terminal primer containing phenylalanine to alanine mutations at AA 705 and 707. Catalytically inactive Pol $\eta$  was generated by mutating codons D13, E22, D115 and E116 to alanine in the N-terminal catalytic active site to disrupt coordination of Mg<sup>2+</sup> ions between dNTP, primer and active site moieties and block nucleotide incorporation(40); this construct was then cloned into pACCMV using EcoRI and BamHI restriction sites. N-terminal Pol $\eta$  truncations were generated with 5' and 3' primers containing EcoRI and BamHI restriction sites, respectively, and cloned into pACCMV. The Rad18–Pol $\eta$  fusion was constructed by PCR amplification of Pol $\eta$  with primers containing 3' BamHI and 5' XbaI restriction sites, followed by ligation into pACCMV–Rad18. Pol $\eta$ - $\Delta$ PLTH and Polk+PLTH were generated with C-terminal primers omitting or adding, respectively, codons for the PLTH domain, followed by a BamHI restriction site for ligation into pACCMV. pDEST-SFB-Spartan was obtained from Lee Zou (MGH Cancer Center). Adenovirus constructions were performed by recombination of pACCMV constructs with pJM17 as described previously (41).

### Adenoviral expression and titration

Adenoviral infection was performed as described previously by adding to cultured cells CsCl-purified adenovirus (41). Infections in H1299 cells were typically done at 0.1–1.0  $\times 10^9$  pfu/ml and in XPV/HDF cells at 0.1–5.0  $\times 10^9$  pfu/ml. Titration to expression levels approximately equal to endogenous was done by serial infections followed by immunoblotting of extracts with antibodies against the endogenous protein.

### Fluorescence microscopy

H1299 or XPV cells were grown to ~60% confluency on glass-bottom plates (Mat-tek) and then infected with adenovirus (CFP–Rad18–WT, YFP–Pol $\eta$ , GFP–Polk and respective mutants) to achieve expression approximately equal to endogenous as determined by Western blot. For co-expression and knockdown experiments, co-infection or transfection was performed 6 h before adenoviral infection. Twenty hours after infection, cells were exposed to genotoxins and then prepared for live or fixed-cell imaging on a Zeiss 710 confocal microscope. For high-magnification representative images, Z-stacks at 0.5- $\mu$ m intervals were collected throughout the entire cell volume using a 63 $\times$  oil-immersion objective and 2.3 $\times$  optical zoom. 3D projections of Z-stacks were performed

using Grouped Zprojector on ImageJ. For cells expressing multiple chromophores (YFP and CFP-tagged proteins), appropriate excitation lasers, laser intensities and emission filter bandwidths were selected to eliminate bleedthrough. For live-cell imaging, cells were kept out of the incubator for no more than 10 min. For fixed-cell imaging, H1299 cells were washed 3× with cold phosphate-buffered saline (PBS), then extracted for 60 s in cold CSK buffer, washed 3× with PBS, then fixed for 10 min in 2% PFA in PBS; XPV cells were washed 3× in cold PBS and then fixed for 15 min in methanol at  $-20^{\circ}\text{C}$ . Post-fixation, all cells were covered with Vectashield Solution (Vector Laboratories) and imaged within 24 h. For foci quantification, five representative images containing ~60 cells were captured using 0.5  $\mu\text{m}$  Z-stacks with a 40× using oil-immersion lens. After 3D projection, the number of cells clearly containing >100 nuclear foci were counted as a fraction of total chromophore-expressing cells.

### Triton extraction, immunoprecipitation and immunoblotting

Extracts containing soluble and chromatin-associated proteins were prepared as previously described (30) by lysing cultured cells into cold cytoskeleton buffer (CSK buffer; 10 mM Pipes, pH 6.8, 100 mM NaCl, 300 mM sucrose, 3 mM  $\text{MgCl}_2$ , 1 mM EGTA, 1 mM DTT, 0.1 mM ATP, 1 mM  $\text{Na}_3\text{VO}_4$ , 10 mM NaF and 0.1% Triton X-100) supplemented with phosphatase and protease inhibitors (Roche Diagnostics, Indianapolis, IN, USA). For immunoprecipitation of whole cell lysate (WCL) or chromatin-bound proteins, Triton-insoluble proteins were released by sonication on ice for three 10-s intervals followed by centrifugation at 15 k  $g$  for 10 min. After normalizing to a protein concentration of 1  $\mu\text{g}/\mu\text{l}$ , immunoprecipitation was conducted at  $4^{\circ}\text{C}$  by rotating overnight with HA-coupled or primary antibody-bound sepharose beads (Roche Diagnostics, Indianapolis, IN, USA). After immunoprecipitation, the beads were washed five times for 15 min in CSK buffer and then resuspended in minimum volume of Laemmli buffer. For immunoblot experiments, cell extracts or immunoprecipitates were separated by SDS-PAGE, followed by incubation overnight with the following primary antibodies: PCNA (sc-56), Chk1 (sc-7898),  $\beta$ -Actin (sc-130656), all from Santa Cruz Biotech (Santa Cruz, CA, USA); Pol $\eta$  (A301–231 A), Pol $\kappa$  (A301–975 A), Pol $\iota$  (A301–304 A) and R18 (A301–340 A), all from Bethyl Laboratories (Montgomery, TX, USA); and p53 (Ab-6) from Lab Vision (Fremont, CA, USA).

### Genotoxin treatments

UV irradiation and benzo(a)pyrene diolepoxide (BPDE) treatment were performed as previously described (30), and BPDE (National Cancer Institute Carcinogen Repository) was dissolved in anhydrous  $\text{Me}_2\text{SO}$  and added directly to the growth medium as a 1000× stock to give various final concentrations, as indicated in the figure legends. For UVC treatment, the growth medium was removed from the cells, reserved and replaced with PBS. The plates were transferred to a UV cross-linker

(Stratagene, Santa Clara, CA, USA) and then irradiated. The UVC dose delivered to the cells was confirmed with a UV radiometer (UVP BioImaging Systems, Upland, CA, USA). The reserved medium from the cells was replaced, and cells were returned to the incubator.

### In vitro binding and ubiquitination assays

C-His<sub>6</sub>-PCNA-expressing Top10 *Escherichia coli* (acquired from Marila Cordiero-Stone, UNC-CH) were collected and lysed in pH 8 buffer containing 50 mM  $\text{NaPO}_4$ , 300 mM NaCl, 20 mM imidazole and 0.1% Triton-X. After sonication and clarification, His<sub>6</sub>-PCNA was purified over Ni-NTA beads. For His<sub>6</sub>-PCNA pulldown experiments, HA-Rad18 was adenovirally expressed in H1299 cells alone or together with YFP-Pol $\eta$  and lysed in  $\text{NaPO}_4/\text{NaCl}/\text{imidazole}/\text{Triton-X}$  buffer. After sonication, clarification and normalization to a protein concentration of 1  $\mu\text{g}/\mu\text{l}$ , cell lysates were rotated overnight at  $4^{\circ}\text{C}$  with His<sub>6</sub>-PCNA on Ni-NTA beads. The beads were then washed five times in the same buffer before addition of Laemmli buffer, boiling and analysis by SDS-PAGE/Western Blot. For *in vitro* ubiquitination assays, H1299 cells expressing HA-Rad18 alone or together with YFP-Pol $\eta$  were lysed in  $\text{NaPO}_4/\text{NaCl}/\text{imidazole}/\text{Triton-X}$  buffer and immunoprecipitated with HA-sepharose beads. After washing the beads extensively, the beads were resuspended in 50  $\mu\text{l}$  buffer and the following were added: His<sub>6</sub>-PCNA (eluted from Ni-NTA beads with the same buffer plus 200 mM imidazole), 500  $\mu\text{M}$  FLAG-ubiquitin, 10× Energy Regeneration Solution and 100 nM Ubiquitin Activating Enzyme (UBE1), all from Boston Biochem (Cambridge, MA, USA). After incubation for 16 h at  $4^{\circ}\text{C}$ , the mixture was mixed with Laemmli buffer, boiled and analysed by SDS-PAGE and Western Blot.

### UV cytotoxicity assay

XPV or HDF cells were split into 24-well plates to a density of ~25%. Twelve hours later, the cells were infected with empty control adenovirus or adenovirus expressing YFP-Pol $\eta$ . Twenty-four hours after infection, the cells were exposed to UV light in the presence or absence of 1 mM caffeine. After 48 h, 50 mg/ml Thiazolyl Blue Tetrazolium Bromide (MTT) (Sigma-Aldrich, St. Louis, MO, USA) was added to each well and allowed to incubate at  $37^{\circ}\text{C}$  for 2 h. The cells were then rinsed with PBS and dissolved in 0.5 ml DMSO. The absorbance at 570 nm was then measured for each well and normalized to the sham-treated samples. The minimum dose of YFP-Pol $\eta$  that conferred resistance to UV light in XPV cells ( $\sim 0.5 \times 10^9$  pfu/ml, Supplementary Figure S2) was determined by this method and used for survival assays.

### Statistics

*P* values for statistical significance were determined by the unpaired Student's *t*-test with a two-tailed 95% confidence interval.

## RESULTS

### Pol $\eta$ promotes efficient Rad18-mediated PCNA monoubiquitination

Current models suggest that Rad18 plays proximal roles in TLS, chaperoning Pol $\eta$  to damaged chromatin and monoubiquitinating PCNA to stably engage Y family polymerases at sites of PRR (12,13). Unexpectedly, we observed deficient redistribution of Rad18 to nuclear foci (representing sites of replication stalling) in patient-derived XPV cells (XP115LO) following UV irradiation (Figure 1A and B, Supplementary Figure S1). In Pol $\eta$ -corrected XP115LO cells, Rad18 redistributed to nuclear foci in a UV-inducible manner and co-localized with Pol $\eta$ , indicating that Rad18 redistribution to repair foci is Pol $\eta$  dependent in XP115LO cells. Similar to results obtained with XPV cells, redistribution of Rad18 was defective in Pol $\eta$ -depleted H1299 cells (Figure 1C and E), which have intact TLS and rely on Pol $\eta$  for UV tolerance (30). As shown in Figure 1D, basal and UV-induced formation of Rad18 foci were dependent on Pol $\eta$ , indicating a general role for Pol $\eta$  in impacting Rad18 redistribution.

We next asked whether Pol $\eta$  status also affected PCNA-directed Rad18 E3 ligase activity. Pol $\eta$ -complemented XPV cells exhibited higher basal and damage-induced PCNA monoubiquitination compared with parental XPV cells, and Pol $\eta$  expression was associated with increased chromatin binding of Rad18 (Figure 1F). Conversely, UV-induced PCNA monoubiquitination was compromised in Pol $\eta$ -depleted normal human diploid fibroblasts (HDF) relative to Pol $\eta$ -replete controls (Figure 1G). Pol $\eta$  depletion thus partially phenocopies the expected effect of depleting RPA (Supplemental Figure S2), which is thought to initiate TLS by coating ssDNA and triggering ATR/Chk1 signalling and subsequent PCNA monoubiquitination (42,43). Rad18 redistribution and PCNA monoubiquitination were also attenuated in Pol $\eta$ -depleted cells after BPDE treatment (Supplementary Figure S3), indicating that the effect of Pol $\eta$  on Rad18 activity is not genotoxin specific.

Next, we determined whether increased Pol $\eta$  expression affects Rad18 and PCNA monoubiquitination. When expressed in HCT-116 cells at levels ranging from ~2- to 25-fold higher than endogenous, PCNA monoubiquitination increased in a dose-dependent fashion with Pol $\eta$  (Figure 1H). Importantly, PCNA monoubiquitination was not induced by Pol $\eta$  in isogenic Rad18-null HCT-116 cells, indicating that the effect of Pol $\eta$  on PCNA modification is Rad18 mediated (Figure 1H, right lane).

Potentially, the stimulatory effect of Pol $\eta$  expression on PCNA monoubiquitination could result (at least in part) from reduced PCNA de-ubiquitylation activity. Ubiquitin-Specific Protease 1 (USP1) is the only known PCNA-directed de-ubiquitylating (DUB) enzyme (44). To determine whether inhibition of USP1 activity contributes to Pol $\eta$ -dependent PCNA monoubiquitination, we determined the effects of Pol $\eta$  expression on PCNA modification in USP1-depleted cells. As expected, basal levels of PCNA monoubiquitination were increased by USP1 depletion (Figure 1H). However, Pol $\eta$  expression further

increased PCNA monoubiquitination in cells lacking USP1 (compare lanes 2 and 8), both basally and 2 and 8 h after DNA damage. We conclude that that Pol $\eta$  stimulates PCNA monoubiquitination by Rad18 via USP1-independent mechanisms. We cannot exclude the formal possibility that Pol $\eta$ -dependent PCNA monoubiquitination is not mediated by reduced activity of putative alternative PCNA-directed DUBs. However, the results of Figure 1 and data presented below indicate that Pol $\eta$  facilitates redistribution of Rad18 to sites of DNA damage and promotes efficient PCNA monoubiquitination.

### Rad18–Pol $\eta$ interaction is necessary for efficient PCNA monoubiquitination

Because Rad18 and Pol $\eta$  form a complex after DNA damage (31), we next asked whether Pol $\eta$ -dependent redistribution of Rad18 and PCNA monoubiquitination required Rad18–Pol $\eta$  interactions. The Pol $\eta$ -binding region of Rad18 has been mapped to amino acid (AA) residues 402–445 (Figure 2A) (31). Therefore, we determined the effect of Pol $\eta$  status on the activity of a Pol $\eta$ -interaction defective Rad18 mutant, Rad18- $\Delta$ (402–445), that retains E3 Ub-ligase activity and other DNA repair functions (31).

Consistent with *in vitro* binding studies (31), Rad18- $\Delta$ (402–445) failed to co-immunoprecipitate Pol $\eta$  from cell lysates (Figure 2B). To test how Pol $\eta$ –Rad18 binding affected subcellular Rad18 distribution, we depleted H1299 cultures of endogenous Rad18 and reconstituted with near-physiological levels of siRNA-resistant CFP-Rad18-WT or CFP-Rad18- $\Delta$ (402–445). As shown in Figure 2C and Supplementary Figure S4, co-expression of Pol $\eta$  significantly increased basal and damage-induced redistribution of Rad18-WT to nuclear foci but had no effect on the redistribution of Rad18- $\Delta$ (402–445). In replicate cultures of Rad18-complemented cells, Pol $\eta$ -induced PCNA monoubiquitination was severely compromised in cells complemented with Rad18- $\Delta$ (402–445) when compared with cells expressing Rad18-WT (Figure 2D, compare lanes 1 and 8 with 11 and 12). Therefore, Pol $\eta$ –Rad18 interactions are necessary for Pol $\eta$ -dependent PCNA monoubiquitination.

The stable engagement of TLS polymerases with stalled replication forks depends on their UBZ/UBM-mediated interactions with monoubiquitinated PCNA (12–14). As expected, the reduced PCNA monoubiquitination in cells complemented with Rad18- $\Delta$ (402–445) was associated with decreased Pol $\eta$  chromatin binding (Figure 2D) and reduced formation of Pol $\eta$  nuclear foci (Figure 2E and F), when compared with Rad18-WT-expressing cells. Thus, Rad18- $\Delta$ (402–445) partially recapitulates phenotypes conferred by the E3 ubiquitin ligase-deficient Rad18-C28F mutant (Figure 2A), including defective PCNA monoubiquitination (Figure 2G) and reduced recruitment of Pol $\eta$  to chromatin (Figure 2E and F).

### Pol $\eta$ –PCNA interactions drive Rad18-mediated PCNA monoubiquitination

C-terminal Pol $\eta$  truncations are the most common defect in XPV (8,45,46), in which both the PIP box (47) and the

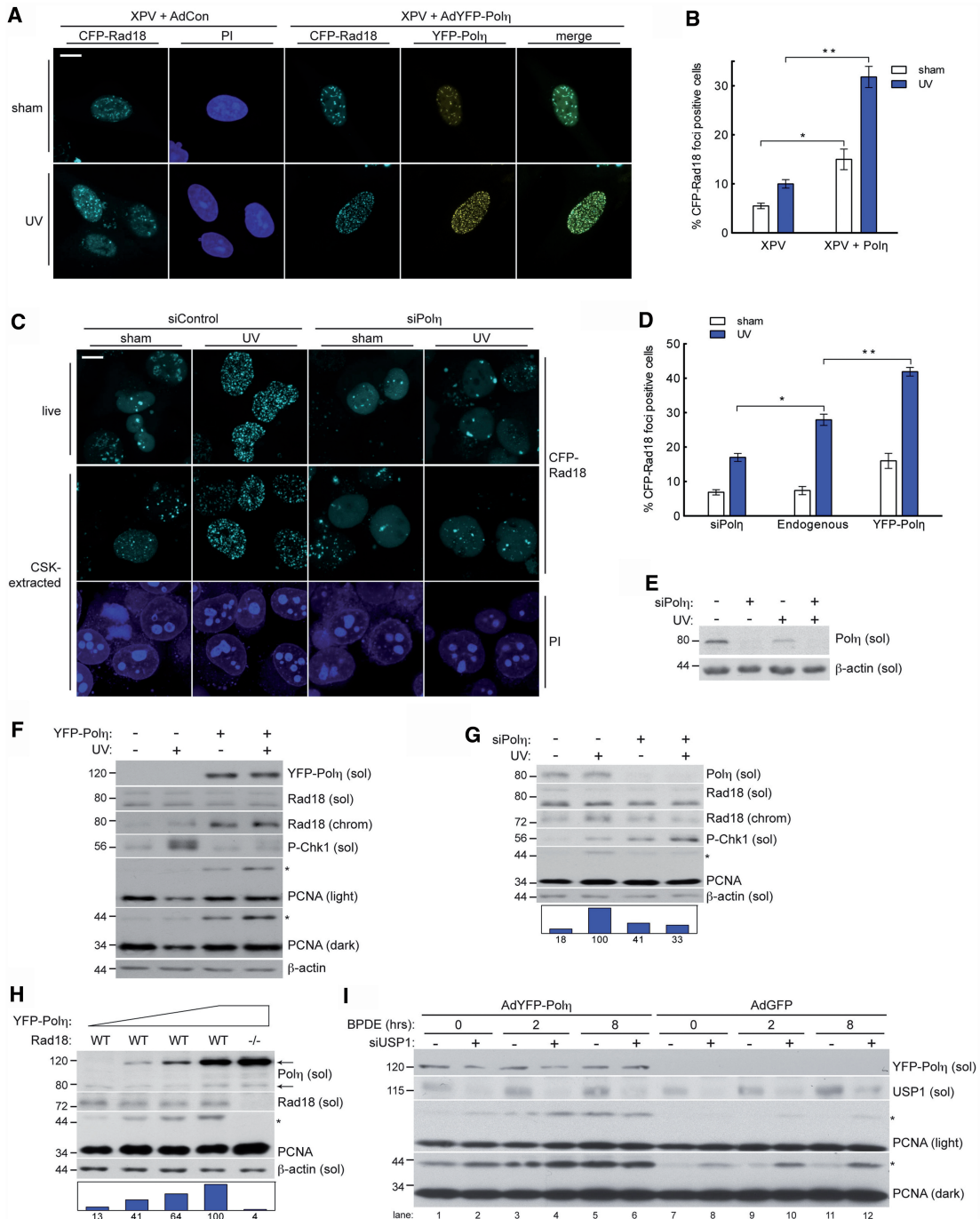


**Figure 1.** Pol $\eta$  promotes damage-induced Rad18 redistribution and PCNA monoubiquitination. (A) Representative images of CSK-extracted nuclei from CFP-Rad18-expressing XP115LO XPV cells co-infected with empty control adenovirus or adenovirus expressing YFP-Pol $\eta$  (at levels that restore UV tolerance—see Supplementary Figure S6) and exposed to UV (10J/m<sup>2</sup>) or sham irradiated. Scalebar = 10  $\mu$ m. (B) Quantification of CFP-Rad18 foci-positive nuclei as a percentage of CFP-Rad18-expressing cells as shown in (A); \**P* = 0.0001; \*\**P* = 0.001. Error bars = SEM. (C) Representative images of live (top) and CSK-extracted (bottom) nuclei from H1299 cells treated with non-targeting control siRNA (left) or siRNA targeting Pol $\eta$  (right) and imaged 2h after sham or UV (10J/m<sup>2</sup>) irradiation. Scalebar = 10 microns. (D) Quantification of CFP-Rad18 foci-positive nuclei as a percentage of CFP-Rad18-expressing cells as shown in (D). \**P* = 0.001; \*\**P* = 0.0003. (E) Immunoblot of fractionated lysates from H1299 cells expressing CFP-tagged Rad18 as shown in (D) and treated with non-targeting control siRNA or siRNA against Pol $\eta$  and then lysed 2h after treatment with 10J/m<sup>2</sup> UV or sham treated. (F) Immunoblot of fractionated lysates from XP115LO XPV cells treated with empty control adenovirus or adenovirus expressing YFP-Pol $\eta$  at levels shown in (A) and lysed 2h after treatment with 10J/m<sup>2</sup> UV. (G) Immunoblot of fractionated lysates from HDF cells treated with non-targeting control siRNA or siRNA against Pol $\eta$  and then lysed 2h after treatment with 10J/m<sup>2</sup> UV or sham irradiation. (H) Immunoblot of fractionated lysates from HCT-116 WT cells (lanes 1–4) or RAD18<sup>-/-</sup> cells (lane 5) treated with increasing titers of YFP-Pol $\eta$  adenovirus and lysed 24h post-infection. Upper and lower arrows denote YFP-tagged and endogenous Pol $\eta$ , respectively. (I) Immunoblot of fractionated lysates from H1299 cells expressing empty control adenovirus or adenovirus expressing YFP-Pol $\eta$  and treated with non-targeting control siRNA or siRNA against USP1 and then lysed at indicated times after treatment with 200nM BPDE. On all Western blots, asterisk denotes monoubiquitinated PCNA and bar graphs represent intensity of monoubiquitinated PCNA band relative to the maximum band on each film.

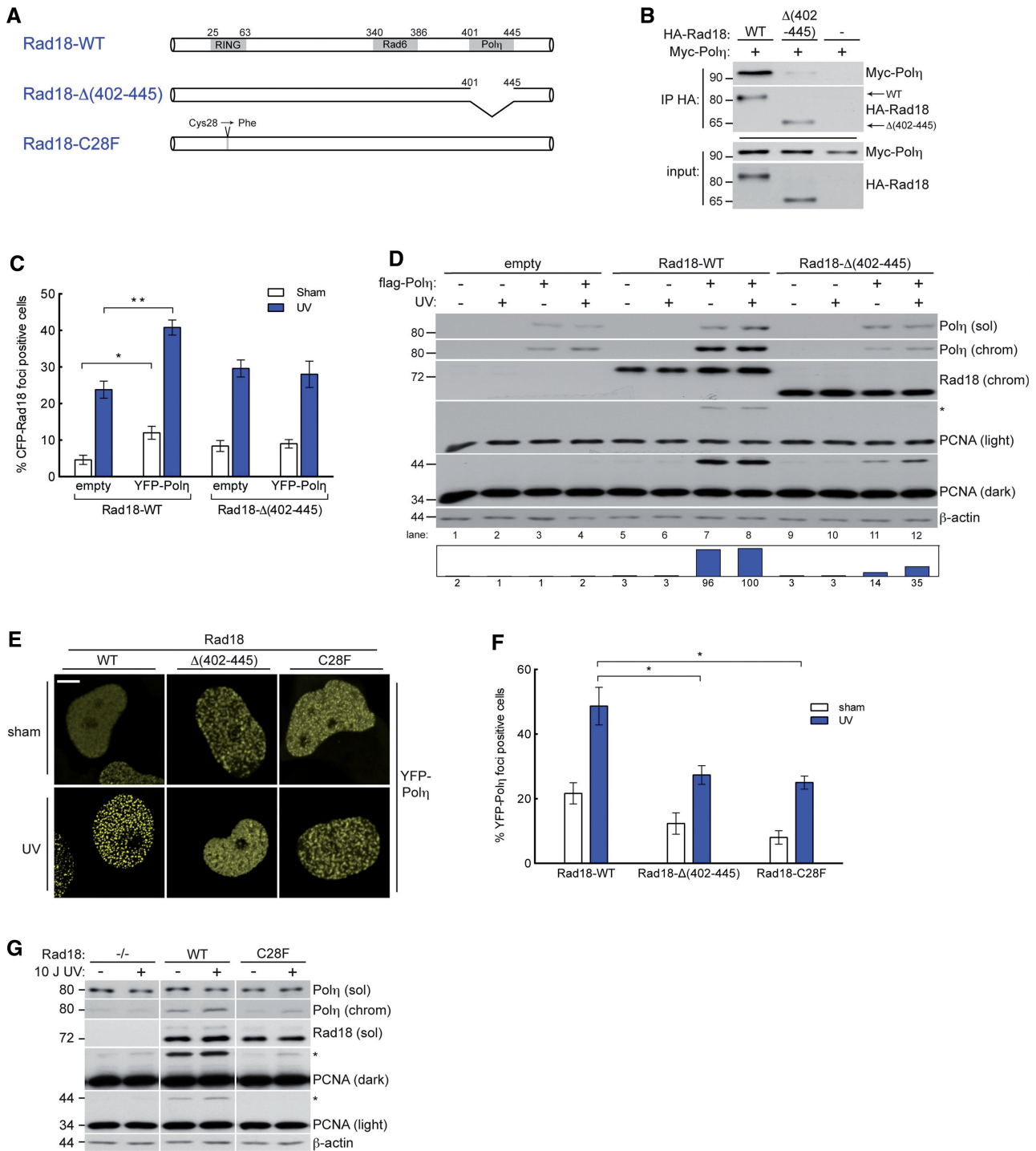


**Figure 2.** Physical interaction between Rad18 and Pol $\eta$  drives efficient damage-induced PCNA ubiquitination. **(A)** Schematic of Rad18-WT (top); Rad18- $\Delta$ (402-445), a Pol $\eta$ -binding deficient mutant lacking the Pol $\eta$  binding domain (AA 402-445); Rad18-C28F, an E3 ligase-inactive mutant in which the RING-finger cysteine has been substituted with phenylalanine. **(B)** Immunoblot analysis of anti-HA immunoprecipitates from H1299 cells co-expressing HA-Rad18-WT or HA-Rad18- $\Delta$ (402-445) with Myc-Pol $\eta$ . **(C)** Quantification of CFP-Rad18 foci-positive nuclei as a percentage of H1299 cells expressing CFP-Rad18-WT or CFP-Rad18- $\Delta$ (402-445) and treated with empty adenovirus or Myc-Pol $\eta$ -expressing adenovirus followed by UV (10J/m<sup>2</sup>) treatment or sham irradiation. \**P* = 0.095; \*\**P* = 0.0006. Error bars = SEM. **(D)** Immunoblots of fractionated lysates from Rad18-depleted H1299 cells that were reconstituted with siRNA-resistant Rad18-WT, Rad18- $\Delta$ (402-445), or empty vector (for control) alone or together with FLAG-Pol $\eta$ , followed by treatment with UV (10J/m<sup>2</sup>) or sham-irradiation. **(E)** Representative images of CSK-extracted nuclei from YFP-Pol $\eta$  expressing H1299 cells that were depleted of endogenous Rad18 and then reconstituted with siRNA-resistant Rad18-WT, or Rad18- $\Delta$ (402-445), or Rad18-C28F and treated with UV (10J/m<sup>2</sup>) or sham irradiated. Scalebar = 10  $\mu$ m. **(F)** Quantification of YFP-Pol $\eta$  foci-positive nuclei as a percentage of YFP-Pol $\eta$ -expressing cells in cultures complemented with Rad18-WT, Rad18- $\Delta$ (402-445), or Rad18-C28F as shown in (E). \*upper *P* = 0.026, lower *P* = 0.0238. **(G)** Immunoblots of fractionated lysates from Rad18-depleted H1299 cells that were reconstituted with siRNA-resistant WT-Rad18, C28F-Rad18, or empty vector, and then treated with UV (10J/m<sup>2</sup>) or sham irradiated.

Rad18-binding domains (31) are deleted. To test whether Pol $\eta$  XPV C-terminal truncation mutants exhibit defects in Rad18 regulation, we complemented XPV cells with WT-Pol $\eta$  or similar levels of a common XPV Pol $\eta$  mutant that retains full catalytic activity (48) but fails to confer UV resistance [Pol $\eta$ - $\Delta$ (1–512), lacking residues 513–713, Figure 3A]. As expected, complementation of XPV cells with Pol $\eta$ -WT conferred normal Rad18 redistribution (Figure 3B and C) and resulted in increased PCNA monoubiquitination (Figure 3D). However, complementation of XPV cells with Pol $\eta$ - $\Delta$ (1–512) failed to restore Rad18 redistribution or PCNA monoubiquitination to the same extent as those complemented with Pol $\eta$ -WT (Figure 2B–D), indicating that the C-terminal domain of Pol $\eta$  is important not only for Pol $\eta$  chromatin binding, but also for Rad18 nuclear redistribution and Rad18-mediated PCNA monoubiquitination.

To test whether loss of PCNA binding contributes to defective PCNA monoubiquitination in Pol $\eta$ - $\Delta$ (1–512)-complemented XPV cells, we generated point mutations in the PIP box that abrogate PCNA binding (47) (Figure 3A). In Rad18-depleted cells complemented with physiological levels of Rad18-WT, Pol $\eta$ -WT, but not Pol $\eta$ - $\Delta$ PIP, promoted PCNA monoubiquitination by Rad18 (Figure 3E, compare lanes 7 and 8 with 11 and 12). Therefore, Pol $\eta$ -PCNA association via the PIP box of Pol $\eta$  contributes to maximal Rad18-mediated PCNA monoubiquitination.

#### Pol $\eta$ scaffolding mediates Rad18–PCNA association

Although Pol $\eta$  possesses a PIP box (47,49) and interacts directly with PCNA (47), no PCNA-interacting domain has been identified for Rad18, and the mechanism for association of Rad18 with PCNA is unknown. The Pol $\eta$  dependence of Rad18-mediated PCNA monoubiquitination (Figures 1–3) suggested that Pol $\eta$  may serve as a ‘molecular bridge’ or scaffold to facilitate Rad18–PCNA interactions. To test this hypothesis, we developed a cell-free system to determine the Pol $\eta$  dependence of PCNA–Rad18 interactions (if any). Recombinant PCNA was immobilized on Ni-NTA beads (or unloaded beads for controls) and incubated with extracts from cells expressing Rad18 alone or in combination with Pol $\eta$ . When extracts from Rad18-expressing cells were incubated with PCNA-Ni beads, we were unable to detect association between Rad18 and PCNA (Figure 3F, lane 1). However, we readily detected Rad18 association with immobilized PCNA incubated with lysates from Rad18 and Pol $\eta$  co-expressing cultures (Figure 3F, lane 2). Therefore, we conclude that Pol $\eta$  promotes Rad18–PCNA interactions or stabilizes Rad18–PCNA complexes.

We modified this cell-free assay to test whether the presence of Pol $\eta$  influenced PCNA monoubiquitination by Rad18. HA-Rad18 was expressed in UV-irradiated H1299 cells individually or in combination with Pol $\eta$  and then immunoprecipitated using anti-HA antibodies. The resulting immune complexes were then mixed with recombinant PCNA, E1, FLAG-ubiquitin and an ATP-regenerating system. As shown in Figure 3G, Rad18 immune complexes conjugated FLAG-ubiquitin to PCNA

in a manner that was stimulated by Pol $\eta$  (compare lanes 2 and 3).

Taken together, the results of Figure 3 suggest that Pol $\eta$  promotes efficient PCNA monoubiquitination via a bridging mechanism that facilitates physical interaction between Rad18 and PCNA.

#### Pol $\eta$ -induced PCNA monoubiquitination is dissociable from catalytic activity

To test whether DNA polymerase activity was required for Pol $\eta$  to promote PCNA monoubiquitination, we generated a Pol $\eta$  mutant harbouring four inactivating point substitutions in conserved residues necessary for catalytic activity (40) (Figure 4A). Catalytically inactive mutant Pol $\eta$  (Pol $\eta$ -C.I.) and wild-type Pol $\eta$  both stimulated PCNA monoubiquitination to similar levels (Figure 4B). Additionally, Pol $\eta$ -C.I. caused Rad18 redistribution to nuclear foci in a manner nearly identical to Pol $\eta$ -WT (Figure 4C and D). Thus, the function of Pol $\eta$  in promoting Rad18-mediated PCNA monoubiquitination is dissociable from its catalytic role as a DNA polymerase.

To probe the molecular determinants of PCNA monoubiquitination induced by Pol $\eta$ , we performed structure–function studies using Pol $\eta$  truncation mutants that progressively eliminated AAs 1–400 spanning the catalytic domain (Figure 4A). Interestingly, when expressed at equal levels, the Pol $\eta$ -truncation mutants mobilized Rad18 to nuclear foci in a manner similar to Pol $\eta$ -WT (Figure 4E). A Pol $\eta$  truncation constituting only 300 C-terminal amino acids induced a level of PCNA monoubiquitination comparable with WT-Pol $\eta$  (Figure 4F). Therefore, the Rad18- and PCNA-binding C-terminus of Pol $\eta$  represents the minimal domain that is necessary and sufficient to regulate Rad18 activity and promote PCNA monoubiquitination.

Recent work identified a novel PIP box and UBZ-containing protein termed ‘Spartan’ that promotes PCNA monoubiquitination via a bridging mechanism between PCNA and Rad18, similar to that which we have defined for Pol $\eta$  (25). To compare the relative contribution of Spartan and Pol $\eta$  to Rad18-mediated PCNA monoubiquitination, we expressed FLAG-Pol $\eta$  or FLAG-Spartan in H1299 cells. When expressed at comparable levels, Pol $\eta$  induced an increase in PCNA monoubiquitination that was nearly 10-fold higher than that conferred by Spartan (Figure 4G) and siRNA-mediated knockdown of Pol $\eta$  decreased UV-induced PCNA monoubiquitination significantly more than Spartan knockdown (Supplementary Figure S5, compare lanes 4 and 6). Together, these data indicate that scaffolding of PCNA and Rad18 by Pol $\eta$  plays an important role in the regulation of PCNA monoubiquitination.

#### Y family polymerase specificity of Pol $\eta$ -dependent PCNA monoubiquitination

We next asked whether the stimulatory effect of Pol $\eta$  on Rad18 activity was shared by other Y-family TLS polymerases. Similar to Pol $\eta$ , Polk associates with Rad18 (41), redistributes to form nuclear foci in response to DNA damage, and associates with PCNA via C-terminal PIP

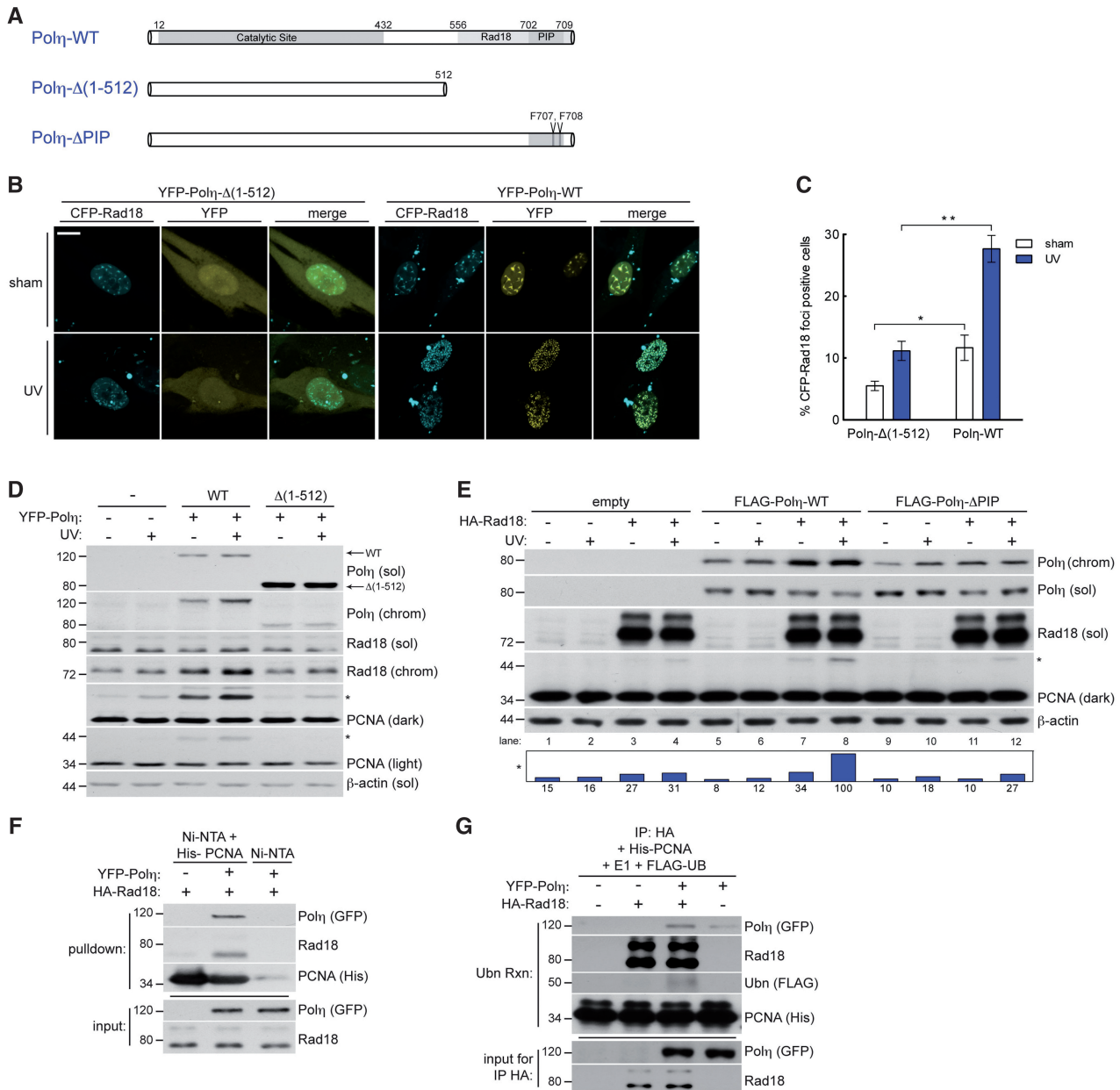


**Figure 3.** Polη physically bridges Rad18 and PCNA to promote efficient PCNA monoubiquitination after DNA damage. (A) Schematic of Polη-WT (top); Polη-Δ(1-512), a C-terminal truncation lacking AA 513-713 (middle); and Polη-ΔPIP, full length Polη with two PIP box phenylalanines mutated to alanine (bottom). (B) Representative images of CSK-extracted nuclei from XPV cells that were co-infected with CFP-Rad18 and YFP-Polη-Δ(1-512) adenovirus (left) or YFP-Polη-WT (right) and treated with UV (10 J/m<sup>2</sup>) or sham irradiated. Scalebar = 10 μm. (C) Quantification of CFP-Rad18 foci-positive nuclei as a percentage of CFP-Rad18-expressing XPV cells expressing YFP-Polη-Δ(1-512) or YFP-Polη-WT adenovirus. \*upper P = 0.018; \*\*P = 0.0001; Error bars = SEM. (D) Immunoblots of fractionated lysates from XPV cells complemented with Polη-WT or Polη-Δ(1-512) and treated with 10 J/m<sup>2</sup> UV. (E) Immunoblots of fractionated lysates from Rad18-depleted H1299 cells that were reconstituted with siRNA-resistant Rad18-WT together with FLAG-tagged Polη-WT or Polη-ΔPIP and treated with sham or 10 J/m<sup>2</sup> UV. (F) *In vitro* pull-down assay. His<sub>6</sub>-PCNA-loaded Nickel beads (or unloaded beads) were incubated with lysates from UV-irradiated H1299 cells expressing HA-Rad18 or both HA-Rad18 and YFP-Polη. (G) *In vitro* ubiquitination assay. HA-Rad18 complexes immunoprecipitated from UV-irradiated H1299 cells expressing HA-Rad18 alone or in combination with YFP-Polη were mixed with recombinant His<sub>6</sub>-PCNA, E1, FLAG-ubiquitin, and an ATP-regenerating system and conjugated FLAG-Ub was detected by immunoblotting with anti-FLAG antibodies.

box. Therefore, for the purpose of comparison with Polη, we determined the effects of manipulating Polk expression levels on PCNA monoubiquitination. In contrast with Polη knockdown, Polk depletion did not attenuate PCNA monoubiquitination basally or after genotoxin treatment (Figure 5A). Even when expressed at levels ~15-fold

higher than Polη, Polk did not induce the robust PCNA monoubiquitination response elicited by Polη (Figure 5B). Polk also induced far less Rad18 redistribution to chromatin. Hence, the role of Polη in promoting genotoxin-induced PCNA monoubiquitination is not shared by all Y-family TLS polymerases.



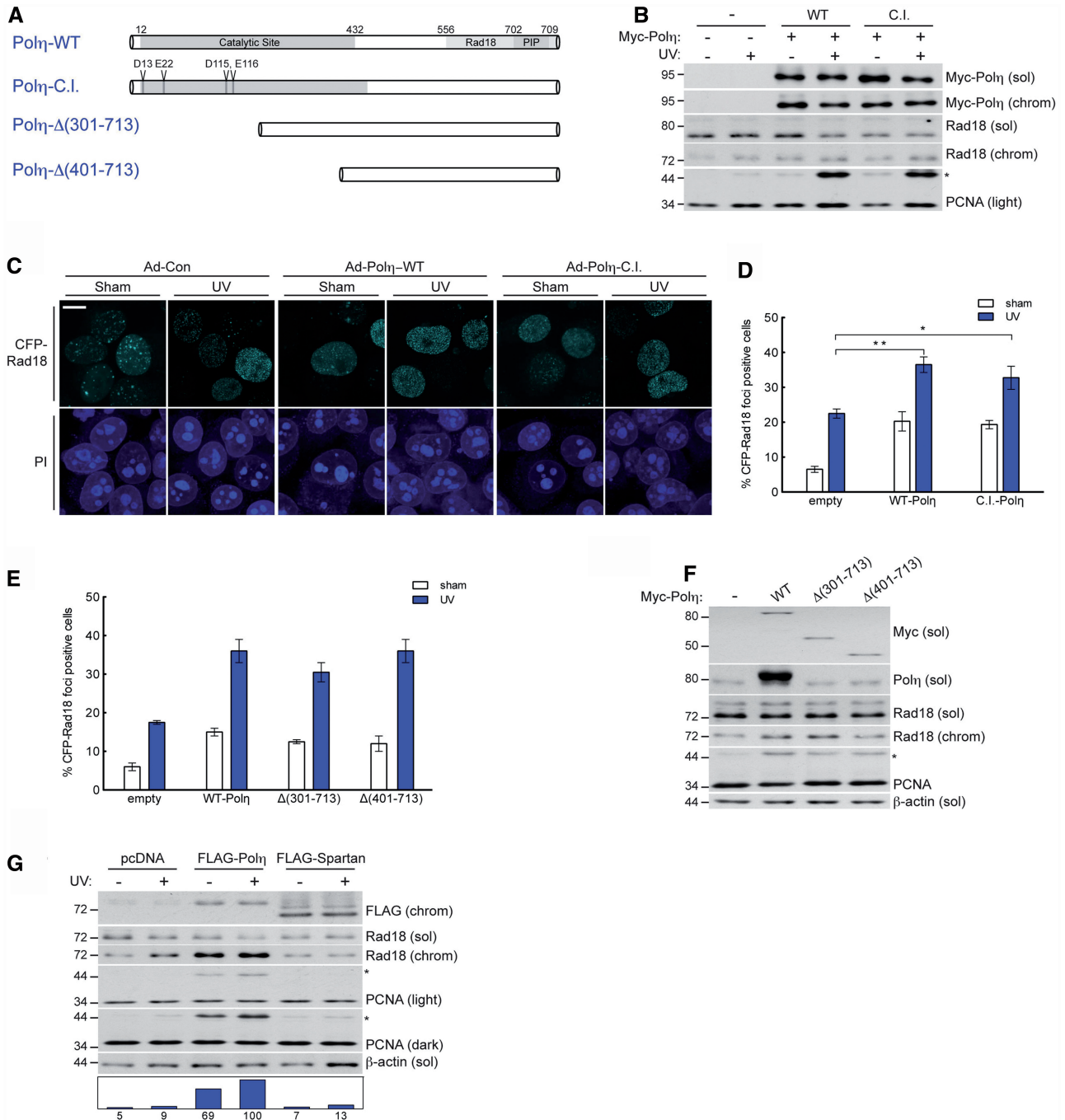


**Figure 4.** Physical bridging of Rad18 and PCNA by Polη is dissociable from its DNA polymerase activity. (A) Schematic of Polη-WT (top); full-length catalytically inactive Polη, Polη-C.I. in which amino acids D13, E22, D115 and E116 are mutated to alanine; and N-terminal Polη truncation mutants, Polη-Δ(301-713) and Polη-Δ(401-713). (B) Immunoblots of fractionated lysates from Myc-Polη-WT or Myc-Polη-C.I.-expressing H1299 cells that were treated with UV (10J/m<sup>2</sup>) or sham irradiated. (C) Representative images of CSK-extracted nuclei from H1299 cells that were co-infected with CFP-Rad18 and empty control adenovirus (left), Myc-Polη-WT (middle) or Myc-Polη-C.I. (right) and treated with UV (10J/m<sup>2</sup>) or sham irradiated. Scalebar = 10 μm. (D) Quantification of CFP-Rad18 foci-positive nuclei as a percentage of CFP-Rad18-expressing H1299 cells expressing empty control adenovirus, Myc-Polη-WT or Myc-Polη-C.I. \*\**P* = 0.0016; \**P* = 0.0287; Error bars = SEM. (E) Quantification of CFP-Rad18 foci-positive nuclei as a percentage of CFP-Rad18-expressing H1299 cells expressing empty control adenovirus, Myc-Polη-WT, Myc-Polη-Δ(301-713) or Myc-Polη-Δ(401-713). Error bars = SEM. (F) Immunoblot of fractionated lysates from H1299 cells expressing empty control adenovirus, Myc-Polη-WT, Myc-Polη-Δ(301-713) or Myc-Polη-Δ(401-713). (G) Immunoblot of fractionated lysates from H1299 cells expressing empty vector control, FLAG-Polη or FLAG-Spartan and lysed 2h after treatment with 10J/m<sup>2</sup> UV or sham treatment.

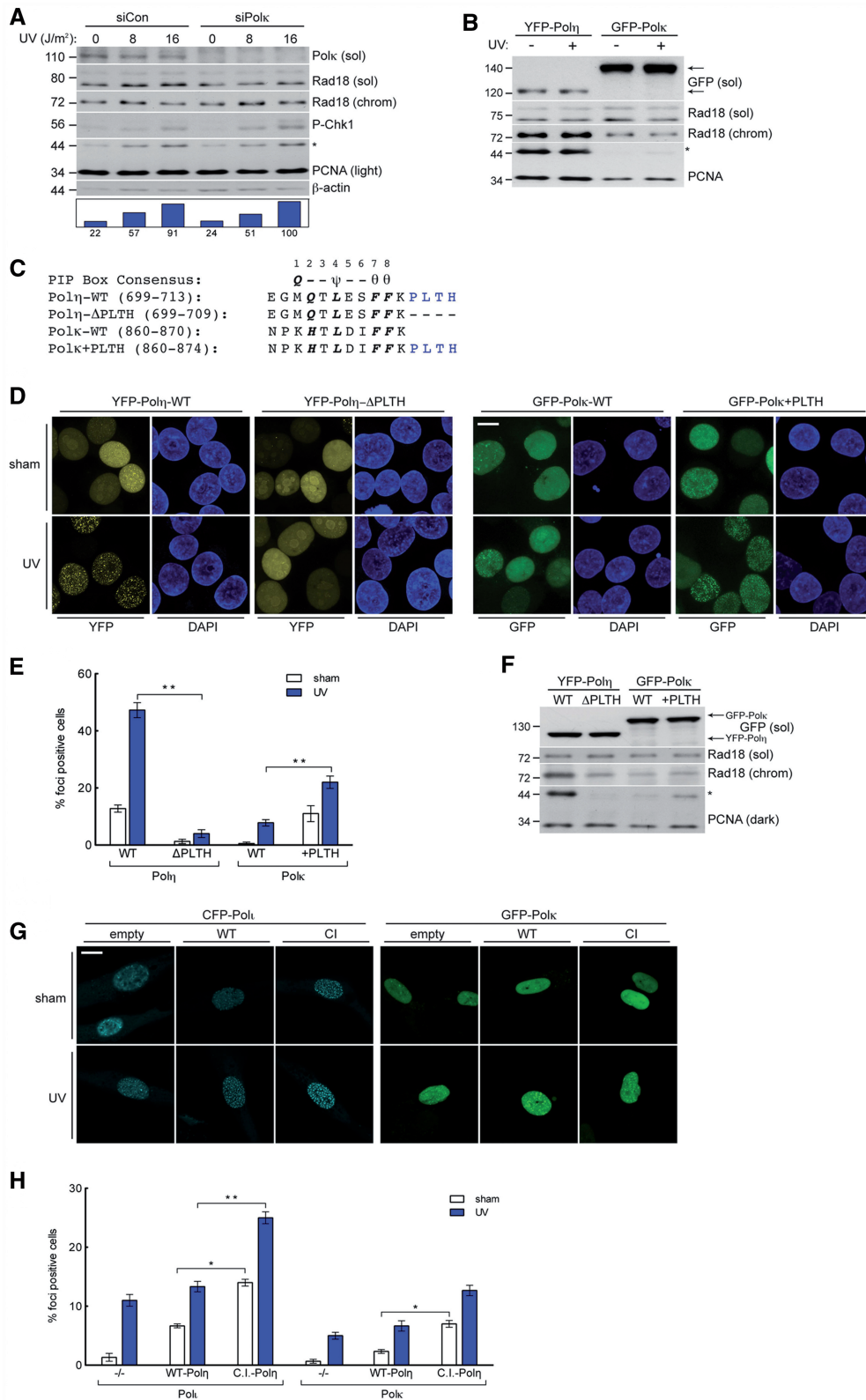


**Figure 5.** High-affinity interaction with PCNA drives Polη-specific induction of PCNA monoubiquitination. (A) Immunoblot of fractionated lysates from control or Polκ-depleted H1299 cells that were lysed 2 h after treatment with UV (10 J/m<sup>2</sup>) or sham irradiation. (B) Immunoblot of fractionated lysates from H1299 cells expressing YFP-Polη or GFP-Polκ and lysed 2 h after treatment with UV (10 J/m<sup>2</sup>) or sham irradiation. (C) Sequence of the C-terminus of Polη and Polκ and the mutants used in domain-swap experiments: Polη-ΔPLTH and Polκ+PLTH. PIP-box consensus amino acids are in bold, where ψ = I/L/M; θ = Y/F. (D) Representative images of CSK-extracted nuclei from H1299 cells that were infected with GFP-Polκ-WT, GFP-Polκ+PLTH, YFP-Polη-WT or YFP-Polη-ΔPLTH and treated with 10 J/m<sup>2</sup> UV or sham irradiated. Scalebar = 10 μm. (E) Quantification of foci-positive nuclei as a percentage of H1299 cells expressing in YFP-Polη-WT, YFP-Polη-ΔPLTH, GFP-Polκ-WT or GFP-Polκ+PLTH.

(continued)

Because Pol $\eta$  and Pol $\kappa$  both associate with Rad18 after DNA damage (30,41), differences in Rad18 binding do not explain the inability of Pol $\kappa$  to promote PCNA monoubiquitination. We therefore hypothesized that differences in TLS polymerase–PCNA binding account for the differential contributions of Pol $\eta$  and Pol $\kappa$  to PCNA monoubiquitination. Domains flanking the PIP boxes in the various Y family members confer dramatically different PCNA-binding affinities (49); specifically, the high PCNA-binding affinity of Pol $\eta$  relative to other TLS polymerases is attributed in large part to the ‘PLTH’ sequence immediately C-terminal to its PIP box (Figure 5C).

To test whether PCNA-binding affinity influences relative PCNA monoubiquitination activity, we performed domain-swap experiments in which we removed the PLTH motif from Pol $\eta$  (generating Pol $\eta$ - $\Delta$ PLTH) or added it to Pol $\kappa$  (generating Pol $\kappa$ +PLTH) (Figure 5C). We then compared the subcellular distribution of wild-type and mutant forms of Pol $\eta$  and Pol $\kappa$ . As expected, Pol $\eta$ - $\Delta$ PLTH showed reduced nuclear focus formation and was also compromised for PCNA monoubiquitination activity relative to Pol $\eta$ -WT (Figure 5D and F). Conversely, whereas Pol $\kappa$ -WT was localized diffusely throughout the nucleus, Pol $\kappa$ +PLTH showed a focal distribution pattern more similar to that of Pol $\eta$ -WT. Interestingly, Pol $\kappa$ +PLTH induced more robust PCNA monoubiquitination than Pol $\kappa$ -WT (Figure 5F), demonstrating that addition of the PLTH (from the Pol $\eta$  PIP) to the Pol $\kappa$  PIP increases its ability to induce PCNA monoubiquitination. Therefore, high affinity binding of Pol $\eta$  to PCNA confers the unique ability among Y-family polymerases to promote PCNA monoubiquitination.

DNA damage-induced PCNA monoubiquitination contributes to the PCNA binding of all Y-family TLS polymerases (11–13). We hypothesized that Pol $\eta$  would influence other Y-family TLS polymerases by facilitating PCNA monoubiquitination, independently of its catalytic activity. Therefore, we compared the UV-inducible redistribution of Pol $\iota$  and Pol $\kappa$  in parental XPV cells or XPV cells reconstituted with Pol $\eta$ -WT or Pol $\eta$ -C.I. Consistent with prior studies (50,51), we found that basal and UV-induced Pol $\iota$  and Pol $\kappa$  redistribution to nuclear foci was higher in Pol $\eta$ -WT-reconstituted XPV cells compared with the Pol $\eta$ -defective parental cell line (Figure 5G and H). Importantly, we found that Pol $\eta$ -C.I. dramatically increased both basal and UV-induced redistribution of Pol $\iota$  and Pol $\kappa$  to nuclear foci. We conclude that cells expressing full-length catalytically inactive Pol $\eta$  retain Rad18-stimulatory activity, which in turn promotes recruitment of alternative error-prone polymerases to stalled replication forks.

### p53 promotes PCNA monoubiquitination via transcriptional induction of Pol $\eta$

Because Rad18-mediated PCNA monoubiquitination was sensitive to Pol $\eta$  expression, it was of interest to determine relative levels of Rad18 and Pol $\eta$  within cells. Therefore, we expressed an in-frame fusion of full-length Pol $\eta$  and full-length Rad18 in cultured cells, which allowed us to perform quantitative comparison of each endogenous protein relative to the Rad18–Pol $\eta$  fusion (Figure 6A) using appropriate antibodies.

At expression levels comparable with endogenous Pol $\eta$ , the Rad18–Pol $\eta$  fusion protein was nearly undetectable in immunoblots with anti-Rad18 antibody (Rad18 light), and prolonged exposures revealed that expression of the fusion at these levels was substantially lower than endogenous Rad18 (Rad18 dark). This surprising result demonstrated that cellular Rad18 protein expression is several orders of magnitude higher than Pol $\eta$  in human cells; we estimate that Rad18 expression exceeds Pol $\eta$  by ~75-fold. Importantly, expression of the Rad18–Pol $\eta$  fusion protein to a level double that of endogenous Pol $\eta$  (and negligible compared with endogenous Rad18) induced a 6-fold increase in PCNA monoubiquitination (right lane), showing that Rad18-mediated PCNA monoubiquitination is highly sensitive to Pol $\eta$  levels. These findings prompted us to determine whether physiologically relevant changes in Pol $\eta$  expression influence PCNA monoubiquitination.

*POLH* is a transcriptional target of activated p53, and DNA damage stimulates p53-dependent increases in Pol $\eta$  protein expression (52). Because endogenous Pol $\eta$  levels are limiting for Rad18 activity, we hypothesized that p53-induced Pol $\eta$  expression contributes to PCNA monoubiquitination. Therefore, we compared UV-induced PCNA monoubiquitination in WT HCT-116 cells and an isogenic p53-null HCT-116 line (Figure 6B). As expected, Pol $\eta$  protein levels were lower in p53-null cells (compared with WT) after UV. Interestingly, PCNA was monoubiquitinated after UV treatment in a manner that was temporally co-incident with Pol $\eta$  expression in p53-expressing HCT-116 cells, but not in p53<sup>-/-</sup> cells.

To test whether the p53-induced PCNA monoubiquitination was Pol $\eta$  dependent, we depleted Pol $\eta$  in p53-null H1299 cells that were transfected with empty vector or pcDNAp53. As shown in Figure 6C, transient expression of p53 led to concomitant increases in Pol $\eta$  expression and UV-induced PCNA monoubiquitination (compare lanes 1 and 2 with 5 and 6). Importantly, Pol $\eta$  depletion severely impaired PCNA monoubiquitination in p53-expressing cells compared to controls. Therefore, the

#### Figure 5. Continued

\*left  $P = 0.0001$ ; \*\* $P = 0.0004$ ; Error bars = SEM. (F) Immunoblot of fractionated lysates from H1299 expressing YFP-Pol $\eta$ -WT, YFP-Pol $\eta$ - $\Delta$ PLTH, GFP-Pol $\kappa$ -WT or GFP-Pol $\kappa$ +PLTH. (G) Representative images of CSK-extracted nuclei from XPV cells that were co-infected with CFP-Pol $\iota$  or GFP-Pol $\kappa$  and empty control adenovirus (left), Myc-Pol $\eta$ -WT (middle) or Myc-Pol $\eta$ -C.I. and treated with UV (10 J/m<sup>2</sup>) or sham irradiated. Scalebar = 10  $\mu$ m. (H) Quantification of CFP-Pol $\iota$  foci-positive nuclei as a percentage of CFP-Pol $\iota$ -expressing XPV cells (left) and GFP-Pol $\kappa$  foci-positive nuclei as a percentage of GFP-Pol $\kappa$ -expressing XPV cells (right), after co-infection with empty control adenovirus, Myc-Pol $\eta$ -WT or Myc-Pol $\eta$ -C.I. and treatment with UV (10 J/m<sup>2</sup>) or sham irradiation. \*left  $P = 0.0009$ ; \*\* $P = 0.0004$ , \*right  $P = 0.0022$ ; Error bars = SEM.

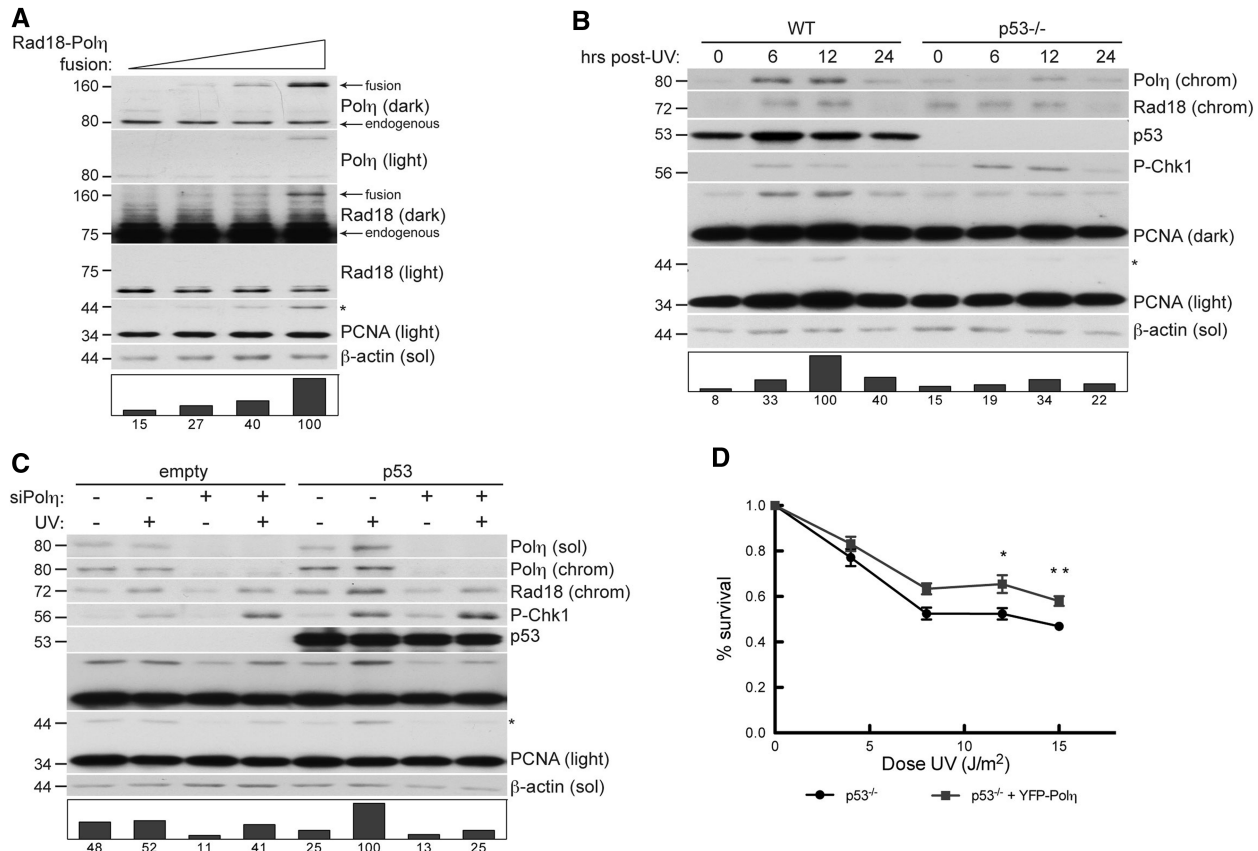


**Figure 6.** Rad18–Pol $\eta$  interaction is checkpoint sensitive and p53 regulated in response to DNA damage. **(A)** Immunoblots of fractionated lysates from H1299 cells transfected with increasing quantities of pACCMV-Rad18-Pol $\eta$  fusion construct. **(B)** Immunoblot of fractionated lysates from HCT-116 WT or HCT-116 p53 $^{-/-}$  cells that were UV treated (30 J/m $^2$ ) and lysed at indicated times after irradiation. **(C)** Immunoblots of fractionated lysates of H1299 cells that were transfected with empty pcDNA as control or pcDNA-p53, followed by non-targeting control siRNA or siRNA against Pol $\eta$ . Cells were lysed 6 h after 10 J/m $^2$  UV. **(D)** UV sensitivity of WT or p53 $^{-/-}$  HDF incubated in 1 mM caffeine and exposed to increasing doses of UV. Cells were infected with YFP-Pol $\eta$  adenovirus at a dose that confers UV survival in XP115LO cells (see Supplementary Figure S6). \*\* $P = 0.0305$  at 12 J/m $^2$ . \*\* $P = 0.0036$  at 15 J/m $^2$ .

p53-dependent component of PCNA monoubiquitination is Pol $\eta$ -mediated.

Because loss of p53 sensitizes normal fibroblasts, but not XPV cells, to UV (53,54), we hypothesized that the UV protection conferred by Pol $\eta$  is mediated by p53. To test this hypothesis, we compared UV survival in p53-depleted HDF cells infected with ‘empty’ control adenovirus or adenovirus expressing Pol $\eta$  at levels that confer UV survival in XPV fibroblasts (Supplementary Figure S6). We found that Pol $\eta$  expression modestly, but significantly, increased UV survival in p53 $^{-/-}$  cells (Figure 6D). Therefore, loss of p53-mediated Pol $\eta$  regulation indeed contributed to the UV sensitivity of p53 null fibroblasts. Together, these results suggest that Pol $\eta$  facilitates PCNA monoubiquitination in a p53-dependent manner, thereby revealing a novel link between the p53 pathway and TLS (Figure 7).

## DISCUSSION

The results described here are consistent with existing models of TLS pathway activation involving an initial redistribution of the Rad18–Pol $\eta$  complex to the vicinity of

damaged DNA (most likely via association of Rad18 with RPA-coated ssDNA) (23,55). However, our results extend current models in that we propose Rad18 is in turn targeted to PCNA, its relevant substrate at the stalled replication fork, by Pol $\eta$  (Figure 7). Specifically, the extreme C-terminus of Pol $\eta$  physically bridges Rad18 and PCNA to stimulate PCNA monoubiquitination (Figure 3), a function unique to Pol $\eta$  among TLS polymerases and fully dissociable from its TLS polymerase activity. The results of this study challenge the notion that TLS constitutes a simple linear pathway in which Rad18 acts upstream of Pol $\eta$  to promote TLS. Instead, we propose that Rad18 and Pol $\eta$  play mutually dependent roles in TLS pathway activation.

Non-catalytic effector functions have been identified for other participants of the DDR, including Rev1 (56), Rad18 (31), NBS1 (57) and Chk1 (58), but this is the first demonstration of a DNA polymerase-independent activity for Pol $\eta$ . A non-catalytic role for Pol $\eta$  in stimulating PCNA monoubiquitination helps explain results of recent studies by other labs. For example, XPV cells are hypersensitive to BPDE and other genotoxins whose DNA lesions are not bypassed by

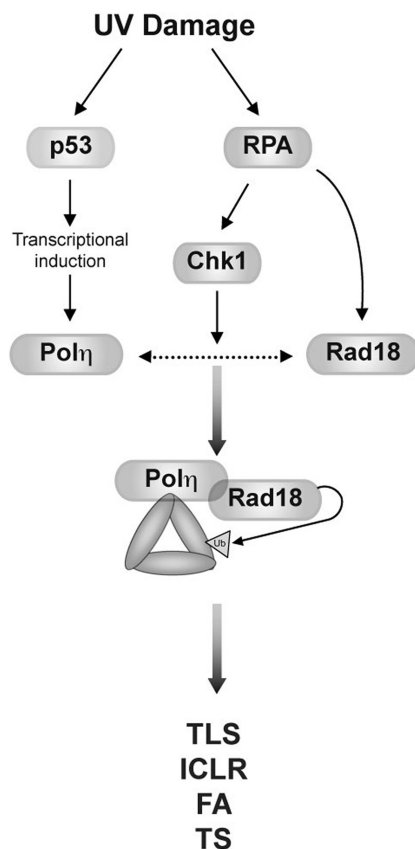


**Figure 7.** Contributions of p53 and Chk1 signalling to Pol $\eta$ -facilitated PCNA monoubiquitination. UV-induced p53 activity leads to transcriptional induction of Pol $\eta$  expression (left). RPA-coated ssDNA generated through helicase-polymerase uncoupling directly recruits Rad18 and promotes Pol $\eta$ -Rad18 association via Chk1 signalling (right), thereby stimulating PCNA monoubiquitination and dependent DDR pathways.

Pol $\eta$  (33,34); clearly, a polymerase-independent function of Pol $\eta$  that promotes PCNA monoubiquitination and activation of Pol $\kappa$  (the TLS polymerase that mediates bypass of BPDE adducts) explains the BPDE sensitivity of XPV cells. In other studies, catalytically dead Pol $\eta$  mutants conferred DNA damage tolerance (36,59) and mutagenesis (35,36). Because PCNA monoubiquitination at K164 is necessary for tolerance of UV and other genotoxins (15–17), restoration of UV survival by catalytically dead Pol $\eta$  (36) is explained by its scaffolding function that promotes PCNA monoubiquitination, thus recruiting other TLS polymerases that facilitate tolerance, albeit at a cost of increased mutagenesis.

The Pol $\eta$  scaffolding function identified here has important implications for the molecular basis of genetic instability in XPV patients. Mutagenesis in XPV cells is widely believed to result solely from deficient Pol $\eta$  polymerase activity (60), leading to error-prone TLS of UV-damaged DNA by alternative and inappropriate TLS polymerases (10). Many XPV mutations encode C-terminally-truncated forms of Pol $\eta$  that lack Rad18- and PCNA-binding domains (45). However, in XPV cells in which Pol $\eta$  catalytic activity is perturbed while Rad18-PCNA bridging activity remains intact, high rates

of UV-induced mutation frequencies may be conferred not only by loss of thymine dimer bypass activity by Pol $\eta$ , but also by stimulation of Rad18-mediated PCNA monoubiquitination and recruitment of alternative error-prone DNA polymerases.

Our finding that cellular Rad18 expression vastly exceeds Pol $\eta$  was unexpected, yet fully explains why PCNA monoubiquitination is exquisitely sensitive to slight alterations in Pol $\eta$  levels (Figure 6). Potentially, any process that affects Pol $\eta$  expression (52), stability (61–63), or nuclear localization (64) or its association with Rad18 is likely to affect PCNA monoubiquitination and in turn influence TLS. Indeed, we show here that transcriptional induction of *POLH* by p53 contributes to PCNA monoubiquitination. The Pol $\eta$ -Rad18 interaction is dependent on checkpoint signalling via Chk1 (30). Therefore, the results of this study may explain the long-standing observation that Chk1 signalling is required for efficient PCNA monoubiquitination (41,58). In fact, the Rad18- $\Delta$ (402–445) mutant in this study that failed to monoubiquitinate PCNA inducibly in response to Pol $\eta$  expression lacks the Chk1-dependent phosphorylation sites required for Pol $\eta$  binding (30). Therefore, the Pol $\eta$ -dependent mechanism for PCNA monoubiquitination described here may provide the basis for cross-talk between TLS and multiple processes including p53 signalling and the S-phase checkpoint.

Several DNA damage-tolerance pathways depend on PCNA monoubiquitination, including replication fork restart (20), template switching (19), intrastrand cross-link repair (21) and the Fanconi Anaemia pathway (22). Hence, Pol $\eta$  contributes to cross-talk between multiple DDR pathways via PCNA monoubiquitination; loss of this element of the DDR in XPV underscores the importance of their orchestrated convergence to preserve genetic stability.

## SUPPLEMENTARY DATA

Supplementary Data are available at NAR Online: Supplementary Figures 1–6.

## ACKNOWLEDGEMENTS

We are grateful to Dr. Hauro Ohmori, Dr. Yuichi Machida and Dr. James Wohlschlegel for helpful discussions. We thank Dr. Marila Cordiero Stone (UNC-CH, USA) for the C-His<sub>6</sub>-PCNA bacterial expression plasmid and XP115LO (XPV) cells. We thank Dr. Bill Kaufmann (UNC-CH, USA) for the WT and p53-depleted HDF. We thank Dr. Lee Zou and Dr. Richard Centore (MGH, USA) for providing Spartan constructs. We are grateful to Dr. Bronwyn M. Gunn for critical reading of the manuscript.

## FUNDING

National Institutes of Health (NIH) [E509558 and E5016280 to C.V. and 1F30ES019449 to M.D.]. Funding for open access charge: NIH [E509558, E5016280].

*Conflict of interest statement.* None declared.

## REFERENCES

- Friedberg, E.C. (2003) DNA damage and repair. *Nature*, **421**, 436–440.
- Friedberg, E.C., Wagner, R. and Radman, M. (2002) Specialized DNA polymerases, cellular survival, and the genesis of mutations. *Science*, **296**, 1627–1630.
- Friedberg, E.C., Fischhaber, P.L. and Kisker, C. (2001) Error-prone DNA polymerases: novel structures and the benefits of infidelity. *Cell*, **107**, 9–12.
- Goodman, M.F. (2002) Error-prone repair DNA polymerases in prokaryotes and eukaryotes. *Annu. Rev. Biochem.*, **71**, 17–50.
- Ohmori, H., Friedberg, E.C., Fuchs, R.P., Goodman, M.F., Hanaoka, F., Hinkle, D., Kunkel, T.A., Lawrence, C.W., Livneh, Z., Nohmi, T. *et al.* (2001) The Y-family of DNA polymerases. *Mol. Cell*, **8**, 7–8.
- Johnson, R.E., Prakash, S. and Prakash, L. (1999) Efficient bypass of a thymine-thymine dimer by yeast DNA polymerase, Poleta. *Science*, **283**, 1001–1004.
- Lehmann, A.R., Kirk-Bell, S., Arlett, C.F., Paterson, M.C., Lohman, P.H., de Weerd-Kastelein, E.A. and Bootsma, D. (1975) Xeroderma pigmentosum cells with normal levels of excision repair have a defect in DNA synthesis after UV-irradiation. *Proc. Natl Acad. Sci. USA*, **72**, 219–223.
- Masutani, C., Kusumoto, R., Yamada, A., Dohmae, N., Yokoi, M., Yuasa, M., Araki, M., Iwai, S., Takio, K. and Hanaoka, F. (1999) The XPV (xeroderma pigmentosum variant) gene encodes human DNA polymerase  $\eta$ . *Nature*, **399**, 700–704.
- Ohashi, E., Ogi, T., Kusumoto, R., Iwai, S., Masutani, C., Hanaoka, F. and Ohmori, H. (2000) Error-prone bypass of certain DNA lesions by the human DNA polymerase  $\kappa$ . *Genes Dev.*, **14**, 1589–1594.
- Wang, Y., Woodgate, R., McManus, T.P., Mead, S., McCormick, J.J. and Maher, V.M. (2007) Evidence that in xeroderma pigmentosum variant cells, which lack DNA polymerase  $\eta$ , DNA polymerase  $\iota$  causes the very high frequency and unique spectrum of UV-induced mutations. *Cancer Res.*, **67**, 3018–3026.
- Freudenthal, B.D., Gakhar, L., Ramaswamy, S. and Washington, M.T. (2010) Structure of monoubiquitinated PCNA and implications for translesion synthesis and DNA polymerase exchange. *Nat. Struct. Mol. Biol.*, **17**, 479–484.
- Kannouche, P.L., Wing, J. and Lehmann, A.R. (2004) Interaction of human DNA polymerase  $\eta$  with monoubiquitinated PCNA: a possible mechanism for the polymerase switch in response to DNA damage. *Mol. Cell*, **14**, 491–500.
- Bienko, M., Green, C.M., Crosetto, N., Rudolf, F., Zapart, G., Coull, B., Kannouche, P., Wider, G., Peter, M., Lehmann, A.R. *et al.* (2005) Ubiquitin-binding domains in Y-family polymerases regulate translesion synthesis. *Science*, **310**, 1821–1824.
- Plosky, B.S., Vidal, A.E., Fernandez de Henestrosa, A.R., McLenigan, M.P., McDonald, J.P., Mead, S. and Woodgate, R. (2006) Controlling the subcellular localization of DNA polymerases  $\iota$  and  $\eta$  via interactions with ubiquitin. *EMBO J.*, **25**, 2847–2855.
- Brown, S., Niimi, A. and Lehmann, A.R. (2009) Ubiquitination and deubiquitination of PCNA in response to stalling of the replication fork. *Cell Cycle*, **8**, 689–692.
- Hendel, A., Krijger, P.H., Diamant, N., Goren, Z., Langerak, P., Kim, J., Reissner, T., Lee, K.Y., Geacintov, N.E., Carell, T. *et al.* (2011) PCNA ubiquitination is important, but not essential for translesion DNA synthesis in mammalian cells. *PLoS Genet.*, **7**, e1002262.
- Krijger, P.H., van den Berk, P.C., Wit, N., Langerak, P., Jansen, J.G., Reynaud, C.A., de Wind, N. and Jacobs, H. (2011) PCNA ubiquitination-independent activation of polymerase  $\eta$  during somatic hypermutation and DNA damage tolerance. *DNA Repair (Amst)*, **10**, 1051–1059.
- Niimi, A., Brown, S., Sabbioneda, S., Kannouche, P.L., Scott, A., Yasui, A., Green, C.M. and Lehmann, A.R. (2008) Regulation of proliferating cell nuclear antigen ubiquitination in mammalian cells. *Proc. Natl Acad. Sci. USA*, **105**, 16125–16130.
- Lin, J.R., Zeman, M.K., Chen, J.Y., Yee, M.C. and Cimprich, K.A. (2011) SHPRH and HLTf act in a damage-specific manner to coordinate different forms of postreplication repair and prevent mutagenesis. *Mol. Cell*, **42**, 237–249.
- Ciccia, A., Nimmonkar, A.V., Hu, Y., Hajdu, I., Achar, Y.J., Izhar, L., Petit, S.A., Adamson, B., Yoon, J.C., Kowalczykowski, S.C. *et al.* (2012) Polyubiquitinated PCNA recruits the ZRANB3 translocase to maintain genomic integrity after replication stress. *Mol. Cell*, **47**, 396–409.
- Yang, K., Moldovan, G.L. and D'Andrea, A.D. (2010) RAD18-dependent recruitment of SNM1A to DNA repair complexes by a ubiquitin-binding zinc finger. *J. Biol. Chem.*, **285**, 19085–19091.
- Geng, L., Huntoon, C.J. and Karnitz, L.M. (2010) RAD18-mediated ubiquitination of PCNA activates the Fanconi anemia DNA repair network. *J. Cell Biol.*, **191**, 249–257.
- Davies, A.A., Huttner, D., Daigaku, Y., Chen, S. and Ulrich, H.D. (2008) Activation of ubiquitin-dependent DNA damage bypass is mediated by replication protein a. *Mol. Cell*, **29**, 625–636.
- Huttner, D. and Ulrich, H.D. (2008) Cooperation of replication protein A with the ubiquitin ligase Rad18 in DNA damage bypass. *Cell Cycle*, **7**, 3629–3633.
- Centore, R.C., Yazinski, S.A., Tse, A. and Zou, L. (2012) Spartan/C1orf124, a reader of PCNA ubiquitylation and a regulator of UV-induced DNA damage response. *Mol. Cell*, **46**, 625–635.
- Davis, E.J., Lachaud, C., Appleton, P., Macartney, T.J., Nathke, I. and Rouse, J. (2012) DVC1 (C1orf124) recruits the p97 protein segregase to sites of DNA damage. *Nat. Struct. Mol. Biol.*, **19**, 1093–1100.
- Juhász, S., Balogh, D., Hajdu, I., Burkovics, P., Villamil, M.A., Zhuang, Z. and Haracska, L. (2012) Characterization of human Spartan/C1orf124, an ubiquitin-PCNA interacting regulator of DNA damage tolerance. *Nucleic Acids Res.*, **40**, 10795–10808.
- Machida, Y., Kim, M.S. and Machida, Y.J. (2012) Spartan/C1orf124 is important to prevent UV-induced mutagenesis. *Cell Cycle*, **11**, 3395–3402.
- Mosbech, A., Gibbs-Seymour, I., Kagias, K., Thorslund, T., Beli, P., Povlsen, L., Nielsen, S.V., Smedegaard, S., Sedgwick, G., Lukas, C. *et al.* (2012) DVC1 (C1orf124) is a DNA damage-targeting p97 adaptor that promotes ubiquitin-dependent responses to replication blocks. *Nat. Struct. Mol. Biol.*, **19**, 1084–1092.
- Day, T.A., Palle, K., Barkley, L.R., Kakusho, N., Zou, Y., Tateishi, S., Verreault, A., Masai, H. and Vaziri, C. (2010) Phosphorylated Rad18 directs DNA polymerase  $\eta$  to sites of stalled replication. *J. Cell Biol.*, **191**, 953–966.
- Watanabe, K., Tateishi, S., Kawasuji, M., Tsurimoto, T., Inoue, H. and Yamaizumi, M. (2004) Rad18 guides poleta to replication stalling sites through physical interaction and PCNA monoubiquitination. *EMBO J.*, **23**, 3886–3896.
- Barkley, L.R., Palle, K., Durando, M., Day, T.A., Gurkar, A., Kakusho, N., Li, J., Masai, H. and Vaziri, C. (2012) c-Jun N-terminal kinase-mediated Rad18 phosphorylation facilitates Poleta recruitment to stalled replication forks. *Mol. Biol. Cell*, **23**, 1943–1954.
- Maher, V.M., McCormick, J.J., Grover, P.L. and Sims, P. (1977) Effect of DNA repair on the cytotoxicity and mutagenicity of polycyclic hydrocarbon derivatives in normal and xeroderma pigmentosum human fibroblasts. *Mutat. Res.*, **43**, 117–138.
- Maher, V.M., Ouellette, L.M., Mittlestat, M. and McCormick, J.J. (1975) Synergistic effect of caffeine on the cytotoxicity of ultraviolet irradiation and of hydrocarbon epoxides in strains of Xeroderma pigmentosum. *Nature*, **258**, 760–763.
- Pavlov, Y.I., Nguyen, D. and Kunkel, T.A. (2001) Mutator effects of overproducing DNA polymerase  $\eta$  (Rad30) and its catalytically inactive variant in yeast. *Mutat. Res.*, **478**, 129–139.
- Ito, W., Yokoi, M., Sakayoshi, N., Sakurai, Y., Akagi, J.I., Mitani, H. and Hanaoka, F. (2012) Stalled Pol $\eta$  at its cognate substrate initiates an alternative translesion synthesis pathway via interaction with REV1. *Genes Cells*, **17**, 98–108.
- Johnson, R.E., Kondratyck, C.M., Prakash, S. and Prakash, L. (1999) hRAD30 mutations in the variant form of xeroderma pigmentosum. *Science*, **285**, 263–265.

38. Pawsey, S.A., Magnus, I.A., Ramsay, C.A., Benson, P.F. and Giannelli, F. (1979) Clinical, genetic and DNA repair studies on a consecutive series of patients with xeroderma pigmentosum. *Q. J. Med.*, **48**, 179–210.
39. Shiomi, N., Mori, M., Tsuji, H., Imai, T., Inoue, H., Tateishi, S., Yamaizumi, M. and Shiomi, T. (2007) Human RAD18 is involved in S phase-specific single-strand break repair without PCNA monoubiquitination. *Nucleic Acids Res.*, **35**, e9.
40. Biertumpfel, C., Zhao, Y., Kondo, Y., Ramon-Maiques, S., Gregory, M., Lee, J.Y., Masutani, C., Lehmann, A.R., Hanaoka, F. and Yang, W. (2010) Structure and mechanism of human DNA polymerase eta. *Nature*, **465**, 1044–1048.
41. Bi, X., Barkley, L.R., Slater, D.M., Tateishi, S., Yamaizumi, M., Ohmori, H. and Vaziri, C. (2006) Rad18 regulates DNA polymerase kappa and is required for recovery from S-phase checkpoint-mediated arrest. *Mol. Cell Biol.*, **26**, 3527–3540.
42. Cimprich, K.A. and Cortez, D. (2008) ATR: an essential regulator of genome integrity. *Nat. Rev. Mol. Cell Biol.*, **9**, 616–627.
43. Zou, L. and Elledge, S.J. (2003) Sensing DNA damage through ATRIP recognition of RPA-ssDNA complexes. *Science*, **300**, 1542–1548.
44. Huang, T.T., Nijman, S.M., Mirchandani, K.D., Galaray, P.J., Cohn, M.A., Haas, W., Gygi, S.P., Ploegh, H.L., Bernards, R. and D'Andrea, A.D. (2006) Regulation of monoubiquitinated PCNA by DUB autocleavage. *Nat. Cell Biol.*, **8**, 339–347.
45. Broughton, B.C., Cordonnier, A., Kleijer, W.J., Jaspers, N.G., Fawcett, H., Raams, A., Garritsen, V.H., Stary, A., Avril, M.F., Boudsocq, F. et al. (2002) Molecular analysis of mutations in DNA polymerase eta in xeroderma pigmentosum-variant patients. *Proc. Natl Acad. Sci. USA*, **99**, 815–820.
46. Tanioka, M., Masaki, T., Ono, R., Nagano, T., Otsu-Honda, E., Matsumura, Y., Takigawa, M., Inui, H., Miyachi, Y., Moriwaki, S. et al. (2007) Molecular analysis of DNA polymerase eta gene in Japanese patients diagnosed as xeroderma pigmentosum variant type. *J. Invest. Dermatol.*, **127**, 1745–1751.
47. Haracska, L., Johnson, R.E., Unk, I., Phillips, B., Hurwitz, J., Prakash, L. and Prakash, S. (2001) Physical and functional interactions of human DNA polymerase eta with PCNA. *Mol. Cell Biol.*, **21**, 7199–7206.
48. Masutani, C., Araki, M., Yamada, A., Kusumoto, R., Nogimori, T., Maekawa, T., Iwai, S. and Hanaoka, F. (1999) Xeroderma pigmentosum variant (XP-V) correcting protein from HeLa cells has a thymine dimer bypass DNA polymerase activity. *EMBO J.*, **18**, 3491–3501.
49. Hishiki, A., Hashimoto, H., Hanafusa, T., Kamei, K., Ohashi, E., Shimizu, T., Ohmori, H. and Sato, M. (2009) Structural basis for novel interactions between human translesion synthesis polymerases and proliferating cell nuclear antigen. *J. Biol. Chem.*, **284**, 10552–10560.
50. Kannouche, P., Fernandez de Henestrosa, A.R., Coull, B., Vidal, A.E., Gray, C., Zicha, D., Woodgate, R. and Lehmann, A.R. (2002) Localization of DNA polymerases eta and iota to the replication machinery is tightly co-ordinated in human cells. *EMBO J.*, **21**, 6246–6256.
51. Sabbioneda, S., Gourdin, A.M., Green, C.M., Zotter, A., Giglia-Mari, G., Houtsmuller, A., Vermeulen, W. and Lehmann, A.R. (2008) Effect of proliferating cell nuclear antigen ubiquitination and chromatin structure on the dynamic properties of the Y-family DNA polymerases. *Mol. Biol. Cell*, **19**, 5193–5202.
52. Liu, G. and Chen, X. (2006) DNA polymerase eta, the product of the xeroderma pigmentosum variant gene and a target of p53, modulates the DNA damage checkpoint and p53 activation. *Mol. Cell Biol.*, **26**, 1398–1413.
53. Wani, M.A., Zhu, Q.Z., El-Mahdy, M. and Wani, A.A. (1999) Influence of p53 tumor suppressor protein on bias of DNA repair and apoptotic response in human cells. *Carcinogenesis*, **20**, 765–772.
54. Laposa, R.R., Feeney, L., Crowley, E., de Feraudy, S. and Cleaver, J.E. (2007) p53 suppression overwhelms DNA polymerase eta deficiency in determining the cellular UV DNA damage response. *DNA Repair (Amst)*, **6**, 1794–1804.
55. Tomida, J., Masuda, Y., Hiroaki, H., Ishikawa, T., Song, I., Tsurimoto, T., Tateishi, S., Shiomi, T., Kamei, Y., Kim, J. et al. (2008) DNA damage-induced ubiquitylation of RFC2 subunit of replication factor C complex. *J. Biol. Chem.*, **283**, 9071–9079.
56. Tissier, A., Kannouche, P., Reck, M.P., Lehmann, A.R., Fuchs, R.P. and Cordonnier, A. (2004) Co-localization in replication foci and interaction of human Y-family members, DNA polymerase pol eta and REV1 protein. *DNA Repair (Amst)*, **3**, 1503–1514.
57. Yanagihara, H., Kobayashi, J., Tateishi, S., Kato, A., Matsuura, S., Tauchi, H., Yamada, K., Takezawa, J., Sugawara, K., Masutani, C. et al. (2011) NBS1 recruits RAD18 via a RAD6-like domain and regulates Pol eta-dependent translesion DNA synthesis. *Mol. Cell*, **43**, 788–797.
58. Yang, X.H., Shiotani, B., Classon, M. and Zou, L. (2008) Chk1 and Claspin potentiate PCNA ubiquitination. *Genes Dev.*, **22**, 1147–1152.
59. Temviriyankul, P., Meijers, M., van Hees-Stuivenberg, S., Boei, J.J., Delbos, F., Ohmori, H., de Wind, N. and Jansen, J.G. (2012) Different sets of translesion synthesis DNA polymerases protect from genome instability induced by distinct food-derived genotoxins. *Toxicol. Sci.*, **127**, 130–138.
60. Lange, S.S., Takata, K. and Wood, R.D. (2011) DNA polymerases and cancer. *Nat. Rev. Cancer*, **11**, 96–110.
61. Jung, Y.S., Liu, G. and Chen, X. (2010) Pirh2 E3 ubiquitin ligase targets DNA polymerase eta for 20S proteasomal degradation. *Mol. Cell Biol.*, **30**, 1041–1048.
62. Jung, Y.S., Qian, Y. and Chen, X. (2012) DNA polymerase eta is targeted by Mdm2 for polyubiquitination and proteasomal degradation in response to ultraviolet irradiation. *DNA Repair (Amst)*, **11**, 177–184.
63. Skoneczna, A., McIntyre, J., Skoneczny, M., Policinska, Z. and Sledziewska-Gojska, E. (2007) Polymerase eta is a short-lived, proteasomally degraded protein that is temporarily stabilized following UV irradiation in *Saccharomyces cerevisiae*. *J. Mol. Biol.*, **366**, 1074–1086.
64. Jung, Y.S., Hakem, A., Hakem, R. and Chen, X. (2011) Pirh2 E3 ubiquitin ligase monoubiquitinates DNA polymerase eta to suppress translesion DNA synthesis. *Mol. Cell Biol.*, **31**, 3997–4006.